Diacetylene Chelator Lipids as Support for Immobilization and Imaging of Proteins by Atomic Force Microscopy

Ingmar T. Dorn,[†,⊥] Ulrich G. Hofmann,[†,||,⊥] Jouko Peltonen,[‡] and Robert Tampé*[,§]

Technische Universität München, Lehrstuhl für Biophysik E22, James-Franck-Strasse, D-85747 Garching, Germany, Åbo Akademi, Institutionen för Fysikalisk Kemi, FIN-20500 Turku, Finland, Max-Planck-Institut für Biochemie, Am Klopferspitz 18a, D-82152 Martinsried, Germany

Received March 10, 1998. In Final Form: May 19, 1998

Chelator lipids represent a powerful and flexible tool to immobilize, orient, and crystallize histidine-tagged proteins at interfaces. To produce stable two-dimensional polymers that are biofunctional, we synthesized diacetylene lipids carrying a metal-chelating headgroup. These lipids were characterized at the air−water interface with respect to their thermodynamic properties, complex formation, and photopolymerization using film balance techniques combined with epi-fluorescence microscopy. Polymerized monolayers were transferred onto solid supports and reversible binding of histidine-tagged protein/DNA complexes was followed by atomic force microscopy. The versatility of the chelator lipid concept may open the possibility to examine structure and function of proteins or multiprotein assemblies under native conditions and in real time by scanning probe microscopy.

Introduction

Modification of surfaces to receive biocompatibility plays an important role in today's biotechnological quest for high-tech assays and novel devices.[1−9] In addition to applications as bioanalytical tools, these biofunctional surfaces were used as substrates for structural investigations of biomolecules by scanning probe microscopy.[10−15] A key technology in this field is the coating of surfaces by stable, ultrathin polymeric films.[16−18] One way to achieve this coating is the formation of self-assembled monolayers of photopolymerizable diacetylene lipid at the air−water interface.[19−23] There is a wealth of data available regarding the unique intrinsic properties of polydiacetylene structures; for examples, a high third-order nonlinear response, a strong dichroism, photoconductivity, low dimensionality, anisotropy, and a triggered fluorescence.[23−31] Most important for coating applications, polymerized diacetylene lipids form stable films so they could be imaged by atomic force microscopy (AFM).[32−37] However, until now, only irreversible protein adsorption

* To whom correspondence should be addressed.
† Technische Universität München.
‡ Åbo Akademi.
§ Max-Planck-Institut für Biochemie.
|| Present address: California Institute of Technology, Division of Biology 216−76, Pasadena, CA 91125.
⊥ Both authors contributed equally to the work.

(1) Swalen, J. D.; Allara, D. L.; Andrade, J. D.; Chandross, E. A.; Garoff, S.; Israelachvili, J.; McCarthy, J. G.; Murray, R.; Pease, R. F.; Rabold, J. F.; Wynne, K. J.; Yu, H. *Langmuir* **1987**, *3*, 932−940.
(2) Gaber, B. P.; Schnur, J. M.; Chapman, D. *Biotechnological applications of lipid microstructures*; Plenum: New York, 1988.
(3) Darst, S. A.; Ahlers, M.; Meller, P.; Kubalek, E. W.; Blankenburg, R.; Ribi, H. O.; Ringsdorf, H.; Kornberg, R. D. *Biophys. J.* **1991**, *59*, 387−396.
(4) Fromherz, P.; Offenhäusser, A.; Vetter, T.; Weis, J. *Science* **1991**, *252*, 1290−1293.
(5) Ribi, H. O. U.S. Patent 4,859, 538, 1989.
(6) Ribi, H. O. U.S. Patent 5,156, 810, 1992.
(7) Ribi, H. O.; Guion, T. A.; Murdoch, J. R.; Scott, J. C.; Pan, V.; Choate, G. L. U.S. Patent 5,427, 915, 1995.
(8) Müller, W.; Ringsdorf, H.; Rump, E.; Wildburg, G.; Zhang, X.; Angermaier, L.; Knoll, W.; Liley, M.; Spinke, J. *Science* **1993**, *262*, 1707−1708.
(9) Spevak, W.; Nagy, J. O.; Charych, D. H.; Schaefer, M. E.; Gilbert, J. H.; Bednarski, M. D. *J. Am. Chem. Soc.* **1993**, *115*, 1146−1147.
(10) Wagner, P.; Hegner, M.; Kernen, P.; Zaugg, F.; Semenza, G. *Biophys. J.* **1996**, *70*, 2052−2066.
(11) Weisenhorn, A.; Drake, B.; Prater, C.; Gould, A.; Hansma, P.; Ohnesorge, F.; Egger, M.; Heyn, S.; Gaub, H. *Biophys. J.* **1990**, *58*, 1251−1258.
(12) Weisenhorn, A.; Schmitt, F.; Knoll, W.; Hansma, P. *Ultramicroscopy* **1992**, *42*, 1125−1132.
(13) Ill, C.; Keivens, V.; Hale, J.; Nakamura, K.; Jue, R.; Cheng, S.; Melcher, E.; Drake, B.; Smith, M. *Biophys. J.* **1993**, *64*, 919−924.
(14) Fritz, M.; Radmacher, M.; Cleveland, J.; Allersma, M.; Stewart, R.; Gieselmann, R.; Janmey, P.; Schmidt, C.; Hansma, P. *Langmuir* **1995**, *11*, 3529−3535.
(15) Müller, D.; Amrein, M.; Engel, A. *J. Struct. Biol.* **1997**, *119*, 172−188.
(16) Ulmann, A. *An introduction to ultrathin organic films*; Academic: San Diego, 1991.
(17) Sackmann, E. *Science* **1996**, *271*, 43−48.
(18) Tampé, R.; Dietrich, C.; Elender, G.; Gritsch, S.; Schmitt, L. *Nanofabrication and Biosystems: Integrating Materials Science, Engeneering, and Biology*; Cambridge University: London, 1996; pp 201−221.
(19) Tieke, B.; Wegner, G.; Nägele, D.; Ringsdorf, H. *Angew. Chem., Int. Ed. Engl.* **1976**, *15*, 764−765.
(20) Bubek, C.; Tieke, B.; Wegner, G. *Ber. Bunsen-Ges. Phys. Chem.* **1982**, *86*, 495−501.
(21) Göbel, H. D.; Gaub, H. E.; Möhwald, H. *Chem. Phys. Lett.* **1987**, *138*, 441−446.
(22) Lieser, G.; Tieke, B.; Wegner, G. *Thin Solid Films* **1980**, *68*, 77−90.
(23) Lochner, K.; Bässler, H.; Tieke, B.; Wegner, G. *Phys. Status Solidi B* **1978**, *88*, 653−658.
(24) Chance, R. R.; Patel, G. N.; Witt, J. D. *J. Chem. Phys.* **1979**, *71*, 206−211.
(25) Eckhardt, H.; Boudreaux, D. S.; Chance, R. R. *J. Chem. Phys.* **1986**, *85*, 4116−4119.
(26) Greene, B. I.; Orenstein, J.; Schmitt-Rink, S. *Science* **1990**, *247*, 679−687.
(27) Patel, G. N.; Witt, J. D.; Khanna, Y. P. *J. Polym. Sci.* **1980**, *18*, 1383−1391.
(28) Roth, S. *One-dimensional metals*; VCH: Weinheim, 1995.
(29) Suzuoki, U.; Kimura, A.; Mizutani, T. *Proceedings of the 7th International Symposium on Electrets*; IEEE: New York, 1991.
(30) Wu, W.-T.; Chen, H.-F. *MRL Bull. Res. Dev.* **1991**, *5*, 1−4.
(31) Charych, D. H.; Nagy, J. O.; Spevak, W.; Bednarski, M. D. *Science* **1993**, *261*, 585−588.
(32) Goettgens, B. M.; Tillmann, R. W.; Radmacher, M.; Gaub, H. E. *Langmuir* **1992**, *8*, 1768−1774.
(33) Radmacher, M.; Goettgens, B. M.; Tillmann, R. W.; Hansma, H. G.; Hansma, P. K.; Gaub, H. E. *Morphology of polymerized membranes on an amorphous substrate at molecular resolution by AFM*; Wichramasinghe, K.; McDonald, F. A.; Eds., American Institute of Physics: New York, 1991.

S0743-7463(98)00284-4 CCC: $15.00
Published on Web 07/23/1998

to polymerized lipid layers was reported.[32,38,39] A more general and reversible protein immobilization technique was recently developed with the application of the metal-chelating group nitrilotriacetic acid or iminodiacetic acid as headgroup of lipids,[40,41] originating from immobilized metal ion affinity chromatography.[42−44] The thermodynamic behavior of these chelator lipids was examined in detail[45−47] and the reversible binding of biomolecules via engineered or surface-exposed histidines to chelator lipid interfaces was demonstrated.[41,48−58]

In this paper we describe the synthesis of a novel polymerizable lipid containing a chelator headgroup for the reversible binding of proteins. This lipid proved to be very useful not only for tailored biocompatible coatings, but even for imaging individual proteins by the scanning force microscope.

Materials and Methods

Materials. All chemicals used in this report were reagent p.a. grade and were checked for purity by thin-layer chromatography (TLC) prior to use. 10,12-Pentacosadiynoic acid was purchased from ABCR (Karlsruhe, Germany), TexasRed-DHPE from Molecular Probes (Eugene, OR), and succinic anhydride from Aldrich (Steinheim, Germany). $N^{\alpha}N^{\alpha}$-Bis(*tert*-butyloxycarbonyl-methylene)-L-lysine-*tert*-butylester was synthesized as described previously.[57] The TLC plates (silica gel 60 F_{254}), silica gel (40−63 μm, 230−400 mesh), bromocresol green, and ninhydrin were from Merck (Darmstadt, Germany). Solvents and all other chemicals were ordered from Fluka (Neu-Ulm, Germany). Solvent ratios are given in volume/volume. All experiments were carried out in *N*-2-hydroxyethylpiperazine-*N*′-ethanesulfonic acid (HEPES) buffer (10 mM HEPES, 50 mM NaCl, pH = 7.0) containing 300 μM $NiCl_2$ or 10 μM ethylenediaminetetraacetic acid (EDTA), respectively.

Analytical Methods. The chemical reactions were monitored by TLC and functional groups were detected on TLC plates by ninhydrin (amines) and bromocresol green (acids and bases). The ^{1}H NMR (500 MHz) and ^{13}C NMR (100 MHz) spectra were recorded on Bruker AM 500 and AM 400 spectrophotometers, respectively. The chemical shifts (δ) are given in ppm relative to the $CDCl_3$ signal. Mass spectrometry (MS) was performed at a Finnigan MAT (Forster City, CA) in the fast-atom bombardment (FAB) ionization mode.

Film Balance Characterization of the Polymerizable Chelator Lipid. The lipid was characterized on a custom-built computerized film balance equipped with a temperature-controlled Teflon trough with an accessible area of 415 × 90 mm^2. Surface tension was measured by a Wilhelmy system with an accuracy of 0.2 mN/m.[59] The velocity of the moveable barrier was computer-controlled (0.08 nm^2 min^{-1} molecule^{-1}). No influence on the area−pressure isotherms were observed at compression rates from 0.04 to 0.08 nm^2 min^{-1} molecule^{-1}. The lipid was dissolved in chloroform/methanol/water (69/27/4) and spread on HEPES buffer containing 300 μM $NiCl_2$ or 10 μM EDTA, respectively.

Fluorescence micrographs were taken on another custom-built film balance. An epi-fluorescence microscope connected to a sensitive camera (SIT, Hamamatsu, Hamamatsu, Japan) was mounted over a small temperature-controlled stationary trough with an accessible surface of 150 × 20 mm^2.[60] A dichroitic-mirror filter set allowing excitation from 530 to 585 nm, and emission of >620 nm (Zeiss IV Fl, Oberkochen, Germany) was used. The light source was a 50 W Hg-lamp (HBO 50, Osram, Germany). Monolayers of the diacetylene chelator lipid were photopolymerized using a light arc lamp (PS300−1, 650 W, ILC Technology, Stanford). The recorded video sequences were digitized by the public domain program NIH−Image[61] on a PowerPC (A/V Macintosh 7100).

Monolayer Transfer on Solid Supports. The 10 × 10-mm^2-sized pieces of silicon wafers with a thermally grown oxide layer of 1800 Å thickness (Wacker Chemitronic, Burghausen, Germany) were thoroughly cleaned prior to use following the procedure described previously.[62] The samples were silanized by dipping the clean substrates for 12 s into a mixture of 80% *n*-hexadecane, 20% chloroform, and 0.1% octadecyltrichlorosilane (OTS) followed by rinsing in pure chloroform. Thereafter, the samples were fixed on magnetic sample holders (double-stick tape, Beiersdorf, Germany) and dipped horizontally through a monolayer spread at the air−water interface into a submerged Petri dish. Care was taken to keep the samples under buffer during the mounting procedure into the AFM.[37] These so-called Langmuir−Schäfer (LS) transfers were carried out on a temperature-controlled Langmuir trough with an accessible area of 450 × 150 mm^2 (KSV 5000, KSV Instruments, Espoo, Finland) in a class 100 clean room hood. Monolayers of ethyl morpholine pentacosadiynoic amide (EMPDA)[35] doped with 10 mol % chelator lipid **6** were polymerized on a water-subphase at 25 mN/m surface pressure (corresponding to ∼28 Å^2/hydrocarbon chain) by UV illumination for 3 min with a 30 W Hg-lamp (λ_{max} = 310 nm).

Atomic Force Microscopy. The AFM measurements were conducted on horizontally LS-transferred monolayers on OTS-hydrophobized silicon-oxide wafers. A Nanoscope III AFM (Digital Instruments, Santa Barbara, CA) with a 150-μm piezo-scanner and microfabricated, oxide-sharpened Si_3N_4 tips (NP−S, Digital Instruments, Santa Barbara, CA) were used. The tips

(34) Radmacher, M.; Zimmermann, R. M.; Gaub, H. E. *Does the scanning force microscope resolve individual lipid molecules?*; Lipowski, R.; Richter, D.; Kremer, K., Eds.; Springer: Berlin, 1992; Vol. 66, pp 24−29.
(35) Sullivan, B.; Kenney, P.; Ribi, H. O.; Hofmann, U. G.; Tillmann, R.; Gaub, H. E. *J. Vac. Sci. Technol. A* **1994**, *12*, 2975−2980.
(36) Tillmann, R. W.; Radmacher, M.; Gaub, H. E.; Kenny, P.; Ribi, H. O. *J. Phys. Chem.* **1993**, *97*, 2928−2932.
(37) Tillmann, R. W.; Hofmann, U. G.; Gaub, H. E. *Chem. Phys. Lipids* **1994**, *73*, 81−89.
(38) Charych, D.; Cheng, Q.; Reichert, A.; Kuziemko, G.; Stroh, M.; Nagy, J.; Spevak, W.; Stevens, R. *Chem. Biol.* **1996**, *3*, 113−120.
(39) Johnson, S. J.; Tillmann, R. W.; Saul, T. A.; Liu, B. L.; Kenney, P. M.; Daulton, J. S.; Gaub, H. E.; Ribi, H. O. *Langmuir* **1995**, *11*, 1257−1360.
(40) Schmitt, L.; Dierich, C.; Tampé, R. *J. Am. Chem. Soc.* **1994**, *116*, 8485−8491.
(41) Shnek, D. R.; Pack, D. W.; Sasaki, D. Y.; Arnold, F. H. *Langmuir* **1994**, *10*, 2382−2388.
(42) Porath, J.; Carlsson, J.; Olsson, I.; Belfrage, G. *Nature* **1975**, *258*, 598−599.
(43) Hochuli, E.; Bannwarth, W.; Döbeli, H.; Gentz, R.; Stüber, D. *Bio/Technology* **1988**, *6*, 1321−1325.
(44) Hochuli, E. *Gen. Eng.* **1990**, *12*, 87−98.
(45) Dietrich, C. Ph.D. Thesis, TU München, 1995.
(46) Pack, D. W.; Arnold, F. H. *Chem. Phys. Lipids* **1997**, *86*, 135−152.
(47) Markowitz, M.; Puranik, D.; Singh, A. *Chem. Phys. Lipids* **1995**, *76*, 63−71.
(48) Dietrich, C.; Schmitt, L.; Tampé, R. *Proc. Natl. Acad. Sci. U.S.A.* **1995**, *92*, 9014−9018.
(49) Gritsch, S.; Neumaier, K.; Schmitt, L.; Tampé, R. *Biosens. Bioelect.* **1995**, *10*, 805−812.
(50) Maloney, K. M.; Shnek, D. R.; Sasaki, D. Y.; Arnold, F. H. *Chem. Biol.* **1996**, *3*, 185−192.
(51) Dietrich, C.; Boscheinen, O.; Scharf, K. D.; Schmitt, L.; Tampé, R. *Biochemistry* **1996**, *35*, 1100−1105.
(52) Barklis, E.; McDermott, J.; Wilkens, S.; Schabtach, E.; Schmid, M. F.; Fuller, S.; Karanjia, S.; Love, Z.; Jones, R.; Rui, Y.; Zhao, X.; Thompson, D. *EMBO* **1997**, *16*, 1199−1213.
(53) Kubalek, E. W.; Le Grice, F. J.; Brown, P. O. *J. Struct. Biol.* **1994**, *113*, 117−123.
(54) Ng, K.; Pack, D. W.; Sasaki, D. Y.; Arnold, F. H. *Langmuir* **1995**, *11*, 4048−4055.
(55) Pack, D. W.; Chen, G.; Maloney, K. M.; Chen, C.; Arnold, F. H. *J. Am. Chem. Soc.* **1997**, *119*, 2479−2487.
(56) Schmitt, L.; Bohanon, T. M.; Denzinger, S.; Ringsdorf, H.; Tampé, R. *Angew. Chem., Int. Ed. Engl.* **1996**, *35*, 317−320.
(57) Dorn, I. T.; Neumaier, K. R.; Tampé, R. *J. Am. Chem. Soc.* **1998**, *120*, 2753−2763.
(58) Bischler, N.; Balavoine, F.; Milkereit, P.; Tschochner, H.; Mioskowski, C.; Schultz, P. *Biophys. J.* **1998**, *74*, 1522−1532.
(59) Tillmann, R. W. Ph.D. Thesis, TU München, 1993.
(60) Heyn, S. P.; Tillmann, R. W.; Egger, M.; Gaub, H. E. *J. Biochem. Biophys. Methods* **1990**, *22*, 145−158.
(61) Rasband, W. *NIH Image*; 1.59 ed.; Rasband, W., Ed.; National Institute of Health: Bethesda, MD, 1995.
(62) Hofmann, U. G.; Tillmann, R. W.; Gaub, H. E. *Polymeric DPDA monolayer on silicon oxide*; Colton, R.; Engel, A.; Frommer, J.; Gaub, H.; Gewirth, A.; Guckenberger, R.; Heckl, W.; Parkinson, B.; Rabe, J.; Eds.; John Wiley & Sons: Sussex, U.K., 1995.

were cleaned prior to use by prolonged UV irradiation. The samples were mounted into the fluid cell of the AFM, where they could be exposed to a subsequent series of buffers. The heat shock factor (HSF24)/DNA complex was assembled with a molar ratio of 2:1 as described[51] and injected into the fluid cell of the AFM to a final protein concentration of 5.7 μg/mL (80 nM HSF/DNA complex) in HEPES buffer containing 300 μM $NiCl_2$ or 10 μM EDTA, respectively. All images were taken in the contact mode with minimal loading force.

Synthesis. *Synthesis of N-tert-Butyloxycarbonyl−diethanolamine **1**.* First, 105 mg (1 mmol) of diethanolamine were dissolved in 30 mL of chloroform, and then 218 mg (1 mmol) of di-*tert*-butyl-dicarbonate in 20 mL chloroform were added under stirring. After completion of the CO_2 production (2 h), the reaction was stopped by addition of 50 mL of hydrochloric acid (pH 2). The phases were separated, the organic phase was dried over anhydrous sodium sulfate, and the solvent as well as the *tert*-butyl alcohol were removed under reduced pressure, yielding 184 mg (0.9 mmol; 90%) of **1**; ^{1}H NMR (400 MHz, $CDCl_3$): δ = 1.46 (s, 9 H, −CO−O−C(C**H**$_3$)$_3$), δ = 3.42 (dd, 4 H, −CO−N((C**H**$_2$)−)$_2$), δ = 3.80 (t, 4 H, −CO−O−C**H**$_2$−); ^{13}C NMR (100 MHz, $CDCl_3$): δ = 29.08, 52.94, 62.54, 80.98, and 157.11; MS (FAB, $C_9H_{19}NO_4$) M+H$^+$-(Boc) = 206 *m/e*.

*Synthesis of N,N-Di-(2-(pentacosa-10,12-diynoyl)oxyethyl)-N-tert-butyloxycarbonylamine **2**.* First, 3.6 mL of a 2 M oxalyl chloride solution in abs. chloroform were added drop by drop to a solution of 678 mg (1.8 mmol) of pentacosadiynoic acid at 0 °C. After 12 h of stirring at room temperature, the chloroform and the excess of oxalyl chloride were evaporated. The crude oil was resolved in 30 mL of abs. chloroform and 200 μL of triethylamine, and then 184 mg (0.9 mmol) of *N-tert*-butyloxycarbonyl−diethanolamine **1** in 20 mL of abs. chloroform were added. The reaction was stirred for 6 h and thereafter extracted twice with 1 N NaOH. The combined organic phases were dried over anhydrous sodium sulfate and the solvent was removed under reduced pressure, yielding 877 mg (0.85 mmol; 94%) of **2**; ^{1}H NMR (400 MHz, $CDCl_3$): δ = 0.89 (t, 6 H, −C**H**$_3$), δ = 1.34 (m, 52 H, $H_3C-(CH_2)_9-$, $-O-CO-(CH_2)_2-(CH_2)_4-$), δ = 1.47 (s, 9 H, −CO−O−C(C**H**$_3$)$_3$), δ =1.51 (q, 8 H, $-C\equiv C-CH_2-CH_2-$), δ = 1.62 (q, 4 H, $-CO-CH_2-CH_2-$), δ = 2.24 (t, 8 H, $-C\equiv C-CH_2-$), δ = 2.30 (t, 4 H, −CO−C**H**$_2$−), δ = 3.50 (dd, 4 H, −CO−N(−(C**H**$_2$)−)$_2$), δ = 4.18 (t, 4 H, −CO−O−C**H**$_2$−); ^{13}C NMR (100 MHz, $CDCl_3$): δ = 14.78, 19.91, 23.38, 25.55, 29.07, 29.48, 29.59, 29.80, 30.04, 30.18, 30.32, 32.61, 34.90, 47.69, 62.96, 63.18, 65.98, 66.07, 80.94, 155.89, and 174.23; MS (FAB, $C_{59}H_{99}NO_6$) M+H$^+$-(Boc) = 818 *m/e*.

*Synthesis of N,N-Di-(2-(pentacosa-10,12-diynoyl)oxyethyl)-amine **3**.* First, 877 mg (0.85 mmol) of **2** were dissolved in 20 mL of chloroform/trifluoroacetic acid (TFA) (4/1) and stirred for 4 h at room temperature. Thereafter, the solution was extracted twice with 1 N NaOH. The combined organic phases were dried over anhydrous sodium sulfate and the solvent was evaporated under reduced pressure, yielding 690 mg (0.84 mmol; 99%) of **3**; ^{1}H NMR (400 MHz, $CDCl_3$): δ = 0.89 (t, 6 H, −C**H**$_3$), δ = 1.33 (m, 52 H, $H_3C-(CH_2)_9-$, $-O-CO-(CH_2)_2-(CH_2)_4-$), δ = 1.51 (q, 8 H, $-C\equiv C-CH_2-CH_2-$), δ = 1.62 (q, 4 H, $-CO-CH_2-CH_2-$), δ = 2.23 (t, 8 H, $-C\equiv C-CH_2-$), δ = 2.32 (t, 4 H, −CO−C**H**$_2$−), δ = 2.90 (t, 4 H, HN(−(C**H**$_2$)−)$_2$), δ = 4.18 (t, 4 H, −CO−O−C**H**$_2$−); ^{13}C NMR (100 MHz, $CDCl_3$): δ = 14.78, 19.91, 23.38, 25.62, 29.05, 29.48, 29.59, 29.81, 30.04, 30.18, 30.33, 32.62, 34.92, 48.72, 64.33, 65.98, 66.08, and 174.40; MS (FAB, $C_{54}H_{91}NO_4$) M+H$^+$ = 819 *m/e*.

*Synthesis of N,N-Di-(2-(pentacosa-10,12-diynoyl)oxyethyl)-amido-succinyl **4**.* First, 100 mg (1 mmol) of succinic anhydride in 5 mL of chloroform were added drop by drop to a solution of 690 mg (0.84 mmol) of **3** and 200 μL of triethylamine in 30 mL of chloroform. After stirring for 4 h at room temperature, the solution was extracted with 1 N NaOH and 1 N hydrochloric acid. The organic phases were combined and dried over anhydrous sodium sulfate, and the solvent was removed under reduced pressure, yielding 721 mg (0.78 mmol; 93%) of **4**; ^{1}H NMR (400 MHz, $CDCl_3$): δ = 0.88 (t, 6 H, −C**H**$_3$), δ = 1.27 (m, 52 H, $H_3C-(CH_2)_9-$, $-O-CO-(CH_2)_2-(CH_2)_4-$), δ =1.51 (q, 8 H, $-C\equiv C-CH_2-CH_2-$), δ = 1.59 (q, 4 H, $-O-CO-CH_2-CH_2-$), δ = 2.23 (t, 8 H, $-C\equiv C-CH_2-$), δ = 2.30 (t, 4 H, −CO−C**H**$_2$−), δ = 2.70 (m, 4H, $-CO-(CH_2)_2-COOH$), δ = 3.62 (dd, 4 H, −CO−N(−(C**H**$_2$)−)$_2$), δ = 4.21 (t, 4 H, −CO−O−C**H**$_2$−); ^{13}C NMR (100 MHz, $CDCl_3$): δ = 14.76, 19.88, 23.35, 25.47, 28.67, 29.05, 29.46, 29.56, 29.77, 30.01, 30.15, 30.30, 32.59, 34.67, 34.80, 46.44, 47.98, 61.99, 62.51, 65.96, 66.06, 173.00, 174.10, 174.19, 176.90; MS (FAB, $C_{58}H_{95}NO_7$) M + H$^+$ = 919 *m/e*.

*Synthesis of N,N-Di-(2-(pentacosa-10,12-diynoyl)oxyethyl)-amido-succinidiyl-amidobutyl-nitrilotriacetic acid **6**.* First, 93 mg (0.8 mmol) of *N*-hydroxysuccinimide (NHS) in 5 mL of acetone, 164 mg (0.8 mmol) of dicyclohexylcarbodiimide (DCC) in 5 mL of chloroform, and 10 mg of 4-(dimethylamino)pyridine were added to 721 mg (0.78 mmol) of **4**. The solution was stirred overnight at room temperature, the precipitated dicyclohexyl urea was filtered off, and the solvent was evaporated under reduced pressure. The residue was dissolved in 25 mL of chloroform and 200 μL of triethylamine. Then, 327 mg (0.78 mmol) of N^{α},N^{α}-di-*tert*-butylcarboxymethylen-L-lysine-*tert*-butylester **5** in 10 mL of chloroform were added to the solution and stirred for 18 h. Thereafter, 10 mL of TFA were added and the solution was stirred overnight. The solution was extracted twice with 1 N NaOH and dried over anhydrous sodium sulfate, and the solvent was removed under reduced pressure. The product was purified by column chromatography on silica gel with chloroform/methanol/water (69/27/4) as eluant, yielding 614 mg (0.52 mmol; 66%) of **6**; ^{1}H NMR (400 MHz, $CDCl_3$/D_3COD/F_3CCOOD, 3/0.9/0.1): δ = 0.76 (t, 6 H, −C**H**$_3$), δ = 1.24 (m, 56 H, $H_3C-(CH_2)_9-$, $-O-CO-(CH_2)_2-(CH_2)_4-$, $-CO-NH-CH_2-(CH_2)_2-$), δ =1.39 (q, 8 H, $-C\equiv C-CH_2-CH_2-$), δ = 1.49 (q, 4 H, $-O-CO-CH_2-CH_2-$), δ = 1.71 (m, 2 H, $-CO-NH-(CH_2)_3-CH_2-$), δ = 2.11 (t, 8 H, $-C\equiv C-CH_2-$), δ = 2.19 (t, 4 H, −CO−C**H**$_2$−), δ = 2.38, 2.51 (m, 4H, $-CO-(CH_2)_2-COOH$), δ = 3.08 (dd, 2 H, $-CO-NH-CH_2-$), δ = 3.49 (t 1H, $-CH(N(CH_2-COOH)_2)-COOH$), δ = 3.55 (m, 4H, $-CH(N(CH_2COOH)_2)-COOH$), δ = 3.71 (dd, 4 H, $-CO-N((CH_2)-)_2$), δ = 4.21 (t, 4 H, −CO−O−C**H**$_2$−); ^{13}C NMR (100 MHz, $CDCl_3$/D_3COD/F_3CCOOD, 3/0.9/0.1): δ = 14.26, 19.50, 23.06, 23.90, 25.23, 28.79, 28.97, 29.27, 29.50, 29.75, 29.89, 30.04, 32.34, 33.52, 34.53, 45.55, 46.64, 47.78, 55.22, 61.87, 62.28, 62.73, 65.68, 65.78, 173.92, 174.54, 174.81, and 175.42.

Results and Discussion

Synthesis of the Polymerizable Chelator Lipid. Solid-supported films of polymerized diacetylene lipids are well suited for AFM studies because of their flatness and stability toward applied forces. Their applications in scanning probe microscopy can be extended if proteins can be immobilized, oriented, and investigated structurally at these interfaces. Therefore, we designed diacetylene lipids carrying a metal-chelating headgroup that can bind reversibly histidine-tagged fusion proteins upon complexation of nickel ions.

For the synthesis of a polymerizable chelator lipid we coupled the aminobutyl-nitrilotriacetic acid (NTA) synthon **5** via a flexible succinidyl spacer with the polymerizable lipid backbone **3** (Figure 1). The polymerizable lipid moiety was synthesized by coupling of pentacosadiynoic acid with a Boc-protected diethanolamine **1**. Therefore, the diynoic acid was converted to its acid chloride according to Hub et al.[63] The resulting polymerizable lipid **2** was deprotected by TFA and the succinidyl spacer was introduced as previously described.[64] Finally, the *tert*-butyl-protected aminobutyl-NTA **5** was coupled to lipid **4** via DCC/NHS chemistry. Deprotection of the NTA-group by TFA resulted in an overall yield of 52% in the diacetylene chelator lipid **6**.

Monolayer Studies. At the air−water interface lipids and other amphiphiles self-assemble into monolayers and their phase behavior can be analyzed by film balance techniques. Because complexation of nickel ions by the

(63) Hub, H.-H.; Hupfer, B.; Koch, H.; Ringsdorf, H. *Angew. Chem.* **1980**, *92*, 962−964.
(64) Kung, V. T.; Reedemann, C. T. *Biochim. Biophys. Acta* **1986**, *862*, 435−439.

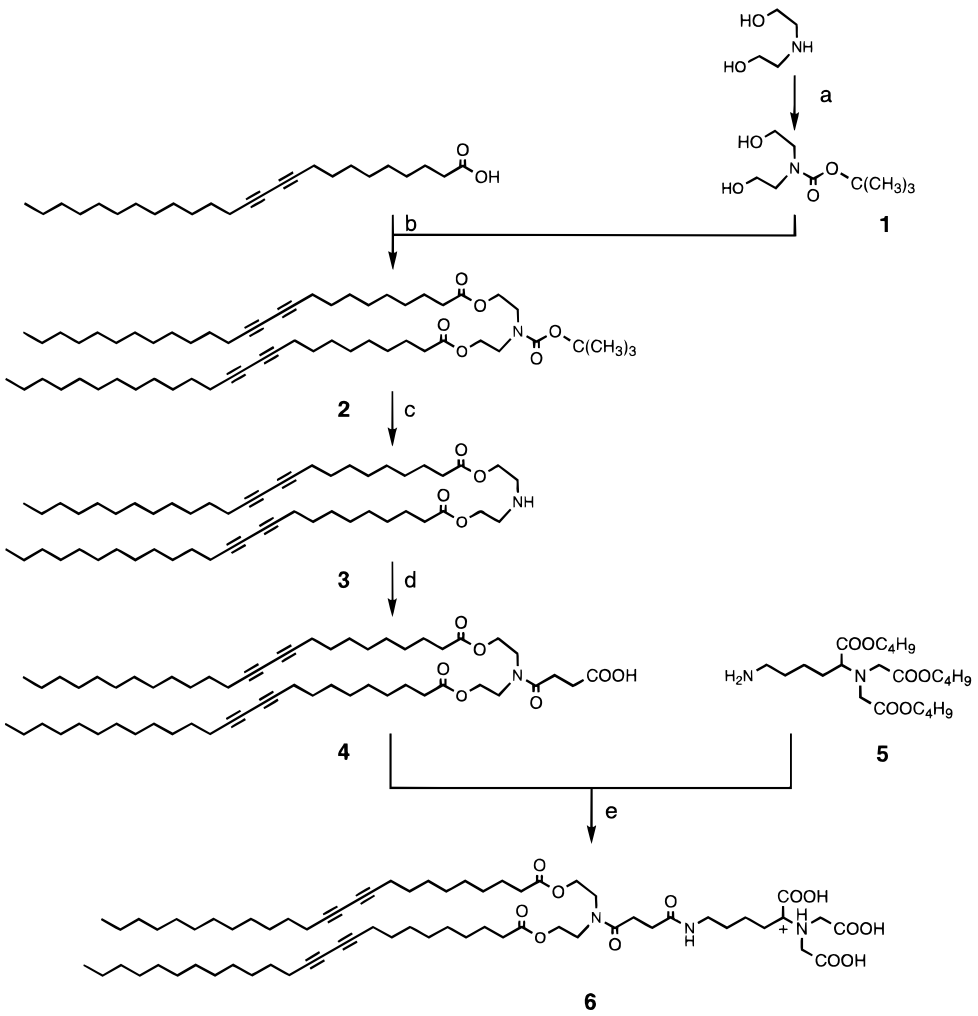

Figure 1. Synthesis of the polymerizable chelator lipid: (a) di-*tert*-butyl-dicarbonate; (b) oxalyl chloride; (c) chloroform/TFA (4/1); (d) succinic anhydride; (e) 1, DCC/NHS, 2, chloroform/TFA (4/1).

chelator lipid **6** has a drastic influence on the charge and geometry of the headgroup, we recorded pressure−area isotherms of the polymerizable chelator lipid **6** at the air−water interface.

In a first set of experiments, the polymerizable chelator lipid was spread onto a HEPES-buffered subphase containing 10 μM EDTA to prevent complex formation by metal ions. The monolayer was stable up to a pressure of 35 mN/m during several cycles of compression and expansion. The pressure−area isotherms show a slight overshoot at the onset of the coexistence region of liquid-expanded and liquid-condensed phases (Figure 2a), which is typical for most diacetylene lipids.[65] This effect is interpreted as a seed-density-dependent supercooling of the two-dimensional fluid.[59] The isotherms show a strong temperature dependence of the coexistence pressure. Phase transition enthalpies were calculated from the two-dimensional Clausius−Clapeyron equation.[66] The transition enthalpies become constant at temperatures below 283 K, whereas they decrease linearly at higher temperatures (Figure 3). The value of 85 kJ/mol at 10 °C is in agreement with published data for other two-chain diacetylene lipids.[65]

In a second set of experiments, the polymerizable chelator lipid was spread onto a HEPES-buffered subphase containing 300 μM $NiCl_2$. In this case, the coexisting pressure was lowered by 14 ± 2 mN/m at the same temperature as compared with the experiments in the absence of nickel ions (Figure 2b). The effects described upon nickel ion complexation are in accordance with the results obtained from chelator lipids with saturated hydrocarbon chains,[40,46] where a lowering of the coexistence pressure of 7 or 10 mN/m, respectively, was observed upon complexation of the metal ion. The effects of complex formation, pH, and ion strength on the chelator lipid monolayer have been previously examined in detail.[45,46] In comparison with the uncomplexed polymerizable chelator lipid, we find only slightly lower transition enthalpies in our experiments and no change in the specific area per molecule of the lipid in the highly condensed state. These results confirmed our assumption that packing of the hydrocarbon chain in the highly condensed phase is not significantly affected by the chelator headgroup.

Under various conditions, phase behavior and polymerization of the lipid monolayers was followed by film balance techniques combined with epi-fluorescence microscopy. First, we investigated domain formation induced by phase separation. Chelator lipid **6** doped with fluorescent lipid was spread onto a HEPES-buffered subphase containing 300 μM $NiCl_2$ and fluorescence micrographs were taken at the onset of the liquid-condensed phase. We observed a temperature-dependent domain shape, starting from small polygons at 5 °C, to wavelike domains

(65) Wagner, D.; Hofmann, U. G.; Dorn, I. T.; Schmitt, L.; Tampé, R.; Gaub, H. E. *Eur. Biophs. J.* **1997**, *26*, 271−275.
(66) Albrecht, O.; Gruler, H.; Sackmann, E. *J. Physique* **1978**, *39*, 301−313.

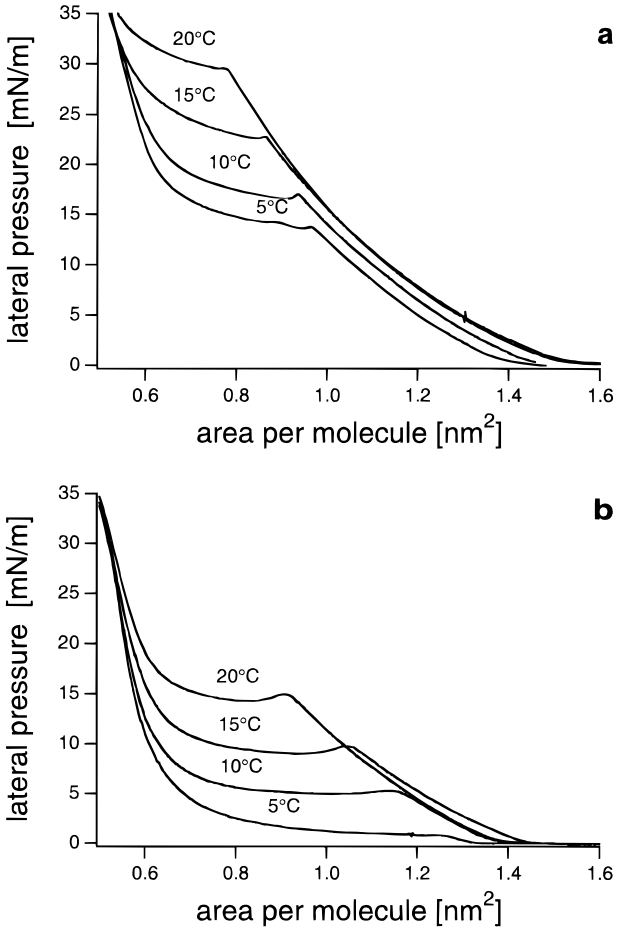

Figure 2. Pressure−area isotherms of the polymerizable chelator lipid **6** at various temperatures on a HEPES buffer containing (a) 10 μM EDTA or (b) 300 μM $NiCl_2$.

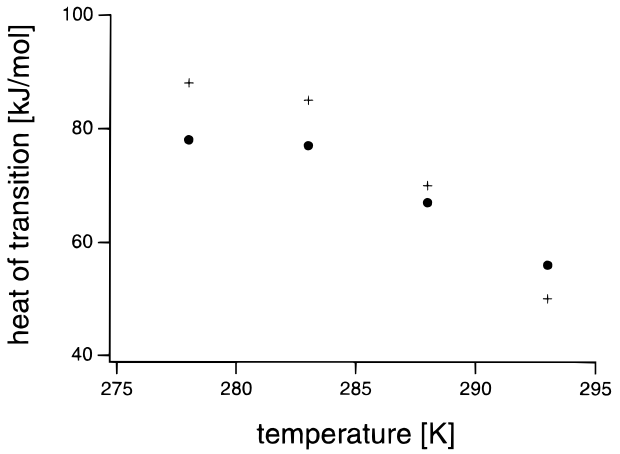

Figure 3. Temperature dependence of the transition enthalpies derived from the isotherms in Figure 2 in the presence of 10 μM EDTA (filled circles) or 300 μM $NiCl_2$ (crosses).

at 10 and 15 °C, and to leaf-like structures at 25 °C (Figure 4). Interestingly, very similar domains were observed for the uncomplexed chelator lipid at the same temperatures (data not shown). This result also gives evidence that the molecular organization of the lipids in the condensed phase is dominated by packing of the hydrocarbon chains and not by the chelator headgroup.

Next, we examined the polymerization of the chelator lipid by epi-fluorescence microscopy because polymerized diacetylene lipids show a strong intrinsic fluorescence emission above 615 nm (excitation 530−585 nm). Therefore, a monolayer of nickel-complexed polymerizable

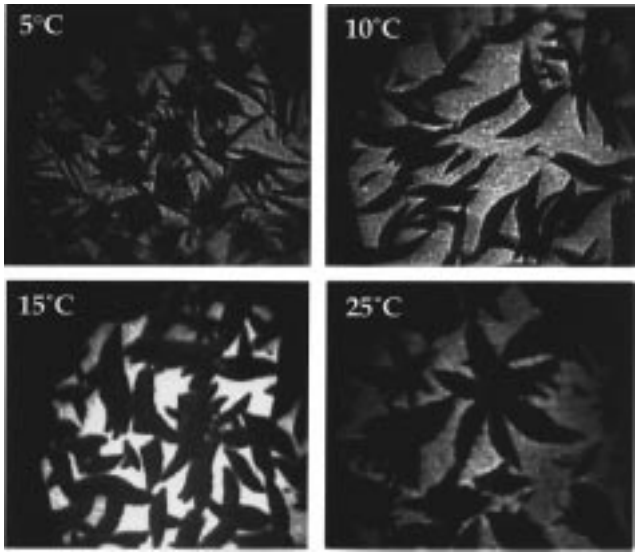

Figure 4. Domain formation induced by phase separation of the polymerizable chelator lipid **6** doped with 0.1 mol % TexasRed-DHPE. Fluorescence micrographs were taken at the onset of the liquid-condensed phase at various temperatures on a HEPES buffer containing 300 μM $NiCl_2$.

chelator lipid was compressed to 35 mN/m and irradiated by a UV lamp for 3 min according to standard protocols.[37,62] In contrast to the general properties of diacetylene lipids, only a weak fluorescence of polymerized chelator lipids was observed, demonstrating that polymerization was inefficient under these conditions (Figure 5a). Longer irradiation of the monolayer did not result in a better degree of polymerization. Because shorter exposure to UV light gave the same results, UV-induced degradation of the polymer can also be excluded.

Surprisingly, longer observation of the monolayer with the fluorescence microscope (excitation from 530 to 585 nm) led to an increasing fluorescence intensity, and bright domains of polymerized lipid were observed after 3 min (Figure 5b). These polymerized domains have a shape similar to those of the liquid-condensed domains observed at the same temperature (Figure 4). Therefore we assume that polymerization occurs preferably in the liquid-condensed domains. This assumption is further supported by photopolymerization of monolayers of lipid **6** doped with fluorescent lipid where the black liquid-condensed domains become bright upon observation with the fluorescence microscope.

An almost uniform fluorescence of the monolayer could be achieved by irradiation (30 min) with white light of a light arc lamp from a distance of 50 cm (Figure 5c). The same results were obtained for the uncomplexed diacetylene chelator lipid monolayer, demonstrating that polymerization is not affected by complex formation of the lipid headgroup.

In both experiments where polymerization was effective, UV light was filtered off by irradiation through a glass slide. A thermal polymerization of the monolayers is also unlikely because no intrinsic fluorescence was observed after longer (3 h) incubation at room temperature. The most plausible explanation is an effective polymerization by visible (VIS) light that is reported very rarely for diacetylene lipids.[20] In contrast to our measurements, these authors find identical polymerization efficiencies by UV and VIS irradiation. The different efficiency of polymerization can either be correlated to distinct spectra and/or different intensities of the light source. Irradiation by the fluorescence microscope occurs only between 530

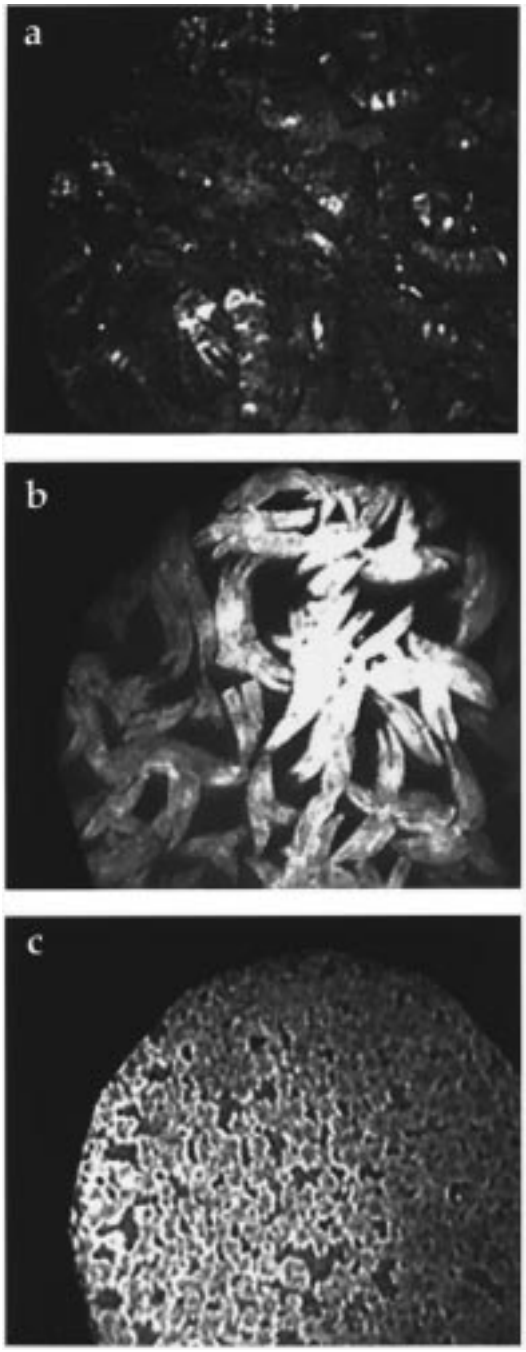

Figure 5. Polymerization of the chelator lipid **6** at the air−water interface. The fluorescence micrographs were taken (30 mN/m lateral pressure) after (a) 3 min of UV irradiation at 10 °C, (b) 3 min of observation with the fluorescence microscope with an excitation of 530−583 nm at 15 °C, and (c) 30 min of irradiation with the light arc lamp at 10 °C. The subphase was HEPES buffer containing 300 μM $NiCl_2$.

and 585 nm, whereas the white spectrum of the light arc lamp contributes also to shorter wavelengths that have been described to be more efficient for photopolymerization of diacetylenes.[67] How the intensity affects the efficiency of polymerization in our experiments is hard to determine because the light arc lamp has a power of 650 W and the microscope lamp has a power of only 50 W, but the power is focused on the illumination spot. Different mechanisms for the VIS light-induced polymerization are discussed in the literature,[67,68] and further investigation of this interesting effect is under way.

AFM Studies. Because the working conditions of an AFM allow for the imaging of single proteins under physiological conditions, we transferred polymerized monolayers onto silanized (OTS) substrates by the LS technique, which appeared to be flat on a large scale. We used monolayers composed of EMPDA, a one-chain polymerizable lipid[35] and 10 mol % polymerizable chelator lipid **6**. Lipids occupy a much smaller area than proteins at interfaces, so these monolayers should present enough active binding sites even for a full coverage of the surface by proteins. The pressure−area isotherms of the mixture did not differ from those of pure EMPDA, if the lateral pressure is plotted against area per hydrocarbon chain instead of area per molecule, providing evidence for ideal mixing. Therefore, a homogeneous distribution of protein binding sites can be assumed. Because EMPDA cannot be photopolymerized efficiently by VIS light, the mixed monolayer was polymerized by UV light (despite the need for VIS light polymerization for the pure lipid **6**) and imaged by contact-AFM after LS transfer. Although the silanized wafer was supposed to be fully covered by the polymer (transfer ratio 100%), we also observed small areas of the uncovered octadecylsilane film (Figure 6a). This result may be due to inhomogeneous photopolymerization of the monolayer so that unpolymerized lipids were washed out after rinsing with buffer containing 0.1% Triton X-100.

Next, the monolayer was flushed by HEPES buffer containing 300 μM $NiCl_2$, which did not affect the appearance of the polymerized monolayer. The AFM allows for imaging adsorption processes onto a surface online, so we injected the histidine-tagged HSF/DNA complex into the fluid cell of the AFM and recorded a time series (Figure 6). Special care was taken to keep the loading force of the tip in the contact mode as low as possible, without loosing contact with the surface. To image single proteins, we chose a low protein concentration of 80 nM. According to a dissociation constant in the micromolar range,[57] the lipid film is far from being covered completely with proteins imaged as round structures (Figure 6). The observed structures consisted of one or more, roughly spherical subunits, as shown in Figure 7, with a maximum thickness of $\sim 3 \pm 0.5$ nm and an apparent diameter of 25 nm. This relatively big diameter for the HSF/DNA complex can be attributed to the known tip broadening.[69,70] Interestingly, most of the protein/DNA complexes are adsorbed at the edges of the polymerized lipid monolayers, which could be due to additional interactions of the proteins with the uncovered silane layer. However, all HSF/DNA molecules are situated at the polymerized monolayer so that specific interaction due to complex binding is dominant.

Unspecific adsorption of the HSF/DNA complex to the uncovered silane layer could be blocked completely by pretreatment of the surface with HEPES buffer containing 0.1% Triton X-100, as seen in Figure 6. To show that the histidine-tagged protein/DNA complex was bound specifically to the nickel-complexed chelator lipid, we performed an identical experiment in the presence of 10 μM EDTA. Even after 60 min, we did not see any adsorption of protein onto the surface, which is in agreement with results of other studies.[48−51,54−57] Moreover, specifically immobilized HSF/DNA complexes dissociated from the surface upon injection of EDTA (10 μM) after 30 min (Figure 6f).

(67) Bubeck, C.; Tieke, B.; Wegner, G. *Ber. Bunsen-Ges. Phys. Chem.* **1982**, *86*, 495−498.
(68) Bara, M.; Schott, M.; Schwoerer, M. *Chem. Phys. Lett.* **1990**, *175*, 23−29.
(69) Radmacher, M.; Fritz, M.; Hansma, H.; PK, H. *Science* **1994**, *265*, 1577−1579.
(70) Henderson, E. *Prog. Surf. Sci.* **1994**, *46*, 39−60.

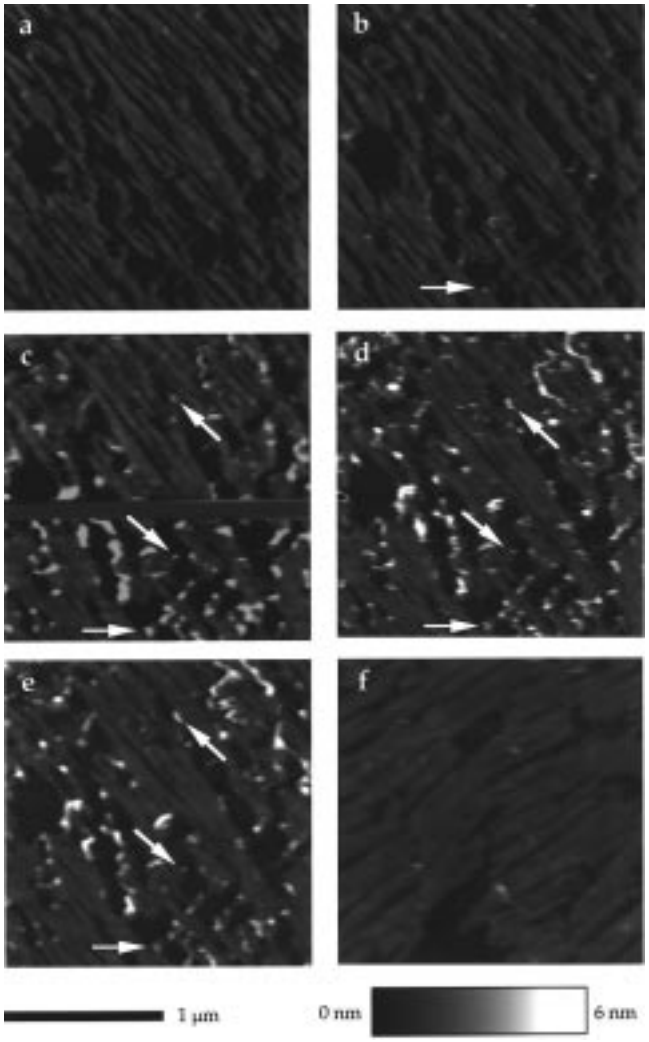

Figure 6. Time series of HSF/DNA complexes (arrows) adsorbing onto a LS-transferred monolayer consisting of 10 mol % chelator lipid **6** and 90 mol % EMPDA. The AFM images were recorded at a protein concentration of 5.7 μg/mL (80 nM HSF/DNA complex) in HEPES buffer containing 300 μM $NiCl_2$ and 0.1% Triton X-100 (a) before injection and after (b) 2 min, (c) 11 min, (d) 13 min, and (e) 32 min. Image (f) was recorded 30 min after rinsing with HEPES buffer containing 10 μM EDTA and 0.1% Triton X-100 at a different area of the lipid layer. Because of the drift upon buffer exchange a different area was imaged. The monolayer was polymerized on a water subphase at 25 mN/m surface pressure (corresponding to ~28 $Å^2$/hydrocarbon chain) by UV illumination for 3 min with a 30 W Hg-lamp with a maximum intensity at 310 nm.

However, because desorption of the HSF/DNA complex took substantially longer than the adsorption, no completely "clean" surface could be imaged under these prolonged imaging conditions (~5 h after the first scanning).

In a previous study, it was demonstrated that histidine-tagged HSF was immobilized functionally at chelator lipid interfaces with respect to its specific DNA recognition.[51] Here, we used a similar approach to show the specific immobilization of the HSF/DNA complex via a histidine tag. Therefore, it could be assumed that the imaged protein/DNA complex remained intact.

To conclude, the reversible immobilization of proteins via an engineered histidine tag onto polymerized chelator lipid layers provides a versatile and powerful technique to image proteins under native conditions with AFM. In contrast to immobilization of histidine-tagged proteins onto nickel adsorbed at mica,[13] the polymerized chelator lipid layer is biocompatible, thereby suppressing unspecific interactions with the surface. Additionally, chelator lipid layers can be transferred onto many different substrates. The resolution of the AFM images can be improved by using tapping mode AFM or by using densely packed protein arrays, which further stabilize the orientation of the scanned object by protein−protein contacts. The major advantage of the chelator lipid concept is the reversible and oriented immobilization of the biomolecule at the interfaces via engineered histidine tags. Therefore, structural and functional studies of individual multimeric protein complexes are challenges for the future. This immobilization technique preserves the functionality of the bound proteins, so imaging of enzymatic activity, molecular motors, or protein motion during catalytic cycles by scanning probe microscopy seems possible.

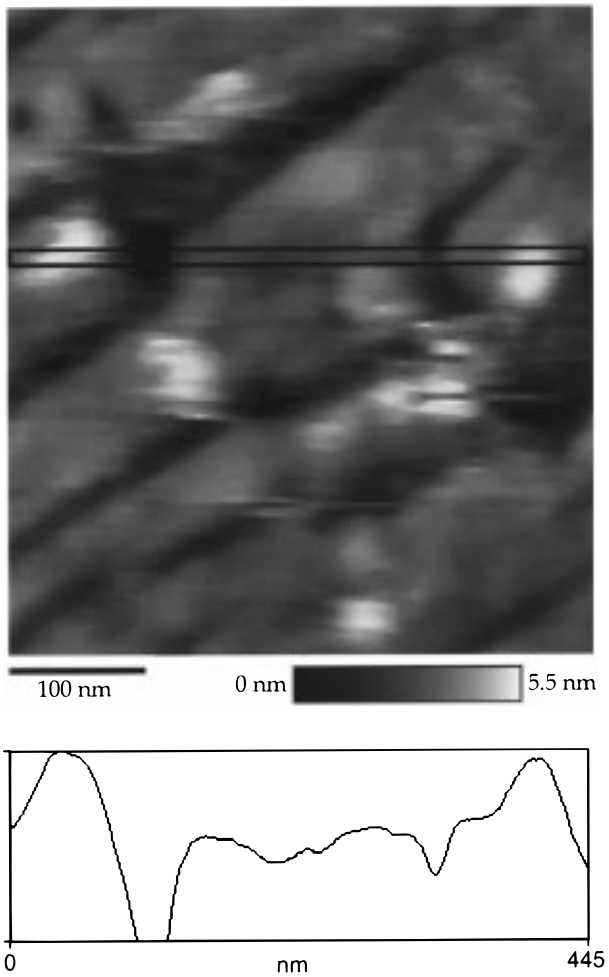

Figure 7. High-resolution AFM image and cross section of HSF/DNA complexes immobilized at the transferred monolayer 60 min after injection (for conditions see Figure 6). The image was taken in contact mode with a NP-S tip with ~2 nN loading force.

Acknowledgment. We thank Hermann Gaub, Walter Häckl, Hans Ribi, Jarl Rosenholm, Erich Sackmann, Lutz Schmitt, and Rudolf Simson for helpful discussions, as well as Wolfram Schäfer and Isolde Sonnenbichler for providing the MS and NMR spectra. We grateful acknowledge Oliver Boscheinen and Klaus-Dieter Scharf for supplying the HSF/DNA complex. This work was supported by the Deutsche Forschungsgemeinschaft and the European Commission (BIOTECH program).

LA980284P